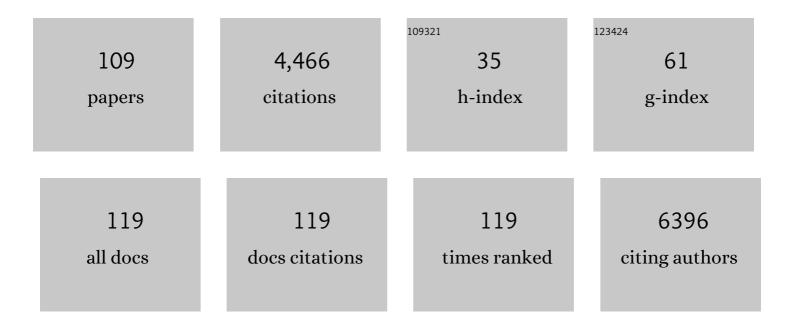
Jerry M Parks

List of Publications by Year in descending order

Source: https://exaly.com/author-pdf/3881768/publications.pdf Version: 2024-02-01



#	Article	IF	CITATIONS
1	The Genetic Basis for Bacterial Mercury Methylation. Science, 2013, 339, 1332-1335.	12.6	778
2	Targeted isolation and cultivation of uncultivated bacteria by reverse genomics. Nature Biotechnology, 2019, 37, 1314-1321.	17.5	231
3	Mutant alcohol dehydrogenase leads to improved ethanol tolerance in <i>Clostridium thermocellum</i> . Proceedings of the National Academy of Sciences of the United States of America, 2011, 108, 13752-13757.	7.1	159
4	Supercomputer-Based Ensemble Docking Drug Discovery Pipeline with Application to Covid-19. Journal of Chemical Information and Modeling, 2020, 60, 5832-5852.	5.4	134
5	AF2Complex predicts direct physical interactions in multimeric proteins with deep learning. Nature Communications, 2022, 13, 1744.	12.8	128
6	Quantum mechanics/molecular mechanics minimum free-energy path for accurate reaction energetics in solution and enzymes: Sequential sampling and optimization on the potential of mean force surface. Journal of Chemical Physics, 2008, 128, 034105.	3.0	110
7	Gram-negative trimeric porins have specific LPS binding sites that are essential for porin biogenesis. Proceedings of the National Academy of Sciences of the United States of America, 2016, 113, E5034-43.	7.1	103
8	Radical Coupling Reactions in Lignin Synthesis: A Density Functional Theory Study. Journal of Physical Chemistry B, 2012, 116, 4760-4768.	2.6	101
9	Down-regulation of the caffeic acid O-methyltransferase gene in switchgrass reveals a novel monolignol analog. Biotechnology for Biofuels, 2012, 5, 71.	6.2	96
10	Reviving Antibiotics: Efflux Pump Inhibitors That Interact with AcrA, a Membrane Fusion Protein of the AcrAB-TolC Multidrug Efflux Pump. ACS Infectious Diseases, 2017, 3, 89-98.	3.8	88
11	Structural Characterization of a Model Gram-Negative Bacterial Surface Using Lipopolysaccharides from Rough Strains of <i>Escherichia coli</i> . Biomacromolecules, 2013, 14, 2014-2022.	5.4	76
12	How to Discover Antiviral Drugs Quickly. New England Journal of Medicine, 2020, 382, 2261-2264.	27.0	76
13	Site-Directed Mutagenesis of HgcA and HgcB Reveals Amino Acid Residues Important for Mercury Methylation. Applied and Environmental Microbiology, 2015, 81, 3205-3217.	3.1	73
14	Mechanism of Hgâ^'C Protonolysis in the Organomercurial Lyase MerB. Journal of the American Chemical Society, 2009, 131, 13278-13285.	13.7	70
15	Liquid crystalline bacterial outer membranes are critical for antibiotic susceptibility. Proceedings of the United States of America, 2018, 115, E7587-E7594.	7.1	67
16	Distribution of mechanical stress in the Escherichia coli cell envelope. Biochimica Et Biophysica Acta - Biomembranes, 2018, 1860, 2566-2575.	2.6	66
17	Quantum Chemical Calculation of p <i>K</i> _a s of Environmentally Relevant Functional Groups: Carboxylic Acids, Amines, and Thiols in Aqueous Solution. Journal of Physical Chemistry A, 2018, 122, 4366-4374.	2.5	62
18	Discovery of critical Tol A-binding residues in the bactericidal toxin colicin N: a biophysical approach. Molecular Microbiology, 1998, 28, 1335-1343.	2.5	58

#	Article	IF	CITATIONS
19	Molecular simulation as a tool for studying lignin. Environmental Progress and Sustainable Energy, 2012, 31, 47-54.	2.3	56
20	Direct visualization of critical hydrogen atoms in a pyridoxal 5′-phosphate enzyme. Nature Communications, 2017, 8, 955.	12.8	55
21	Why Mercury Prefers Soft Ligands. Journal of Physical Chemistry Letters, 2013, 4, 2317-2322.	4.6	54
22	Molecular Properties That Define the Activities of Antibiotics in <i>Escherichia coli</i> and <i>Pseudomonas aeruginosa</i> . ACS Infectious Diseases, 2018, 4, 1223-1234.	3.8	54
23	Benchmark Interaction Energies for Biologically Relevant Noncovalent Complexes Containing Divalent Sulfur. Journal of Physical Chemistry A, 2012, 116, 1086-1092.	2.5	48
24	Inhibitor binding influences the protonation states of histidines in SARS-CoV-2 main protease. Chemical Science, 2021, 12, 1513-1527.	7.4	47
25	X-ray Structure of a Hg ²⁺ Complex of Mercuric Reductase (MerA) and Quantum Mechanical/Molecular Mechanical Study of Hg ²⁺ Transfer between the C-Terminal and Buried Catalytic Site Cysteine Pairs. Biochemistry, 2014, 53, 7211-7222.	2.5	46
26	Chemical Factors that Control Lignin Polymerization. Journal of Physical Chemistry B, 2014, 118, 164-170.	2.6	46
27	β-Barrel proteins tether the outer membrane in many Gram-negative bacteria. Nature Microbiology, 2021, 6, 19-26.	13.3	46
28	Identification and Structure–Activity Relationships of Novel Compounds that Potentiate the Activities of Antibiotics in <i>Escherichia coli</i> . Journal of Medicinal Chemistry, 2017, 60, 6205-6219.	6.4	45
29	Cluster-Continuum Calculations of Hydration Free Energies of Anions and Group 12 Divalent Cations. Journal of Chemical Theory and Computation, 2013, 9, 555-569.	5.3	44
30	Machine Learning Reveals the Critical Interactions for SARS-CoV-2 Spike Protein Binding to ACE2. Journal of Physical Chemistry Letters, 2021, 12, 5494-5502.	4.6	44
31	Experimental Validation of the Docking Orientation of Cdc25 with Its Cdk2â^CycA Protein Substrateâ€. Biochemistry, 2005, 44, 16563-16573.	2.5	43
32	Identification of Mercury and Dissolved Organic Matter Complexes Using Ultrahigh Resolution Mass Spectrometry. Environmental Science and Technology Letters, 2017, 4, 59-65.	8.7	43
33	Hydrolysis of DFP and the Nerve Agent (<i>S</i>)-Sarin by DFPase Proceeds along Two Different Reaction Pathways: Implications for Engineering Bioscavengers. Journal of Physical Chemistry B, 2014, 118, 4479-4489.	2.6	42
34	Longâ€Range Electrostaticsâ€Induced Twoâ€Proton Transfer Captured by Neutron Crystallography in an Enzyme Catalytic Site. Angewandte Chemie - International Edition, 2016, 55, 4924-4927.	13.8	42
35	Environmental Mercury Chemistry – In Silico. Accounts of Chemical Research, 2019, 52, 379-388.	15.6	40
36	Exceptional response and multisystem autoimmune-like toxicities associated with the same T cell		40

#	Article	IF	CITATIONS
37	Direct evidence that an extended hydrogen-bonding network influences activation of pyridoxal 5′-phosphate in aspartate aminotransferase. Journal of Biological Chemistry, 2017, 292, 5970-5980.	3.4	38
38	Molecular Dynamics Simulation of the Structures, Dynamics, and Aggregation of Dissolved Organic Matter. Environmental Science & amp; Technology, 2020, 54, 13527-13537.	10.0	36
39	Direct determination of protonation states and visualization of hydrogen bonding in a glycoside hydrolase with neutron crystallography. Proceedings of the National Academy of Sciences of the United States of America, 2015, 112, 12384-12389.	7.1	35
40	Mercury Methylation by HgcA: Theory Supports Carbanion Transfer to Hg(II). Inorganic Chemistry, 2014, 53, 772-777.	4.0	34
41	Mercury Uptake by <i>Desulfovibrio desulfuricans</i> ND132: Passive or Active?. Environmental Science & amp; Technology, 2019, 53, 6264-6272.	10.0	33
42	Discovery of multidrug efflux pump inhibitors with a novel chemical scaffold. Biochimica Et Biophysica Acta - General Subjects, 2020, 1864, 129546.	2.4	33
43	Structure and Conformational Dynamics of the Metalloregulator MerR upon Binding of Hg(II). Journal of Molecular Biology, 2010, 398, 555-568.	4.2	32
44	A pseudobond parametrization for improved electrostatics in quantum mechanical/molecular mechanical simulations of enzymes. Journal of Chemical Physics, 2008, 129, 154106.	3.0	31
45	Impact of hydration and temperature history on the structure and dynamics of lignin. Green Chemistry, 2018, 20, 1602-1611.	9.0	30
46	Structure determination of the HgcAB complex using metagenome sequence data: insights into microbial mercury methylation. Communications Biology, 2020, 3, 320.	4.4	30
47	Machine learningâ€based prediction of enzyme substrate scope: Application to bacterial nitrilases. Proteins: Structure, Function and Bioinformatics, 2021, 89, 336-347.	2.6	30
48	Substrate Binding Induces Conformational Changes in a Class A β-lactamase That Prime It for Catalysis. ACS Catalysis, 2018, 8, 2428-2437.	11.2	27
49	Identification of Binding Sites for Efflux Pump Inhibitors of the AcrAB-TolC Component AcrA. Biophysical Journal, 2019, 116, 648-658.	0.5	27
50	Exploring Covalent Allosteric Inhibition of Antigen 85C from Mycobacterium tuberculosis by Ebselen Derivatives. ACS Infectious Diseases, 2017, 3, 378-387.	3.8	26
51	Active-Site Protonation States in an Acyl-Enzyme Intermediate of a Class A β-Lactamase with a Monobactam Substrate. Antimicrobial Agents and Chemotherapy, 2017, 61, .	3.2	26
52	Mechanism of Cdc25B Phosphatase with the Small Molecule Substrate <i>p</i> -Nitrophenyl Phosphate from QM/MM-MFEP Calculations. Journal of Physical Chemistry B, 2009, 113, 5217-5224.	2.6	25
53	Multidrug Efflux Pumps and the Two-Faced Janus of Substrates and Inhibitors. Accounts of Chemical Research, 2021, 54, 930-939.	15.6	25
54	Quantum Chemical Characterization of the Reactions of Guanine with the Phenylnitrenium Ion. Journal of Organic Chemistry, 2001, 66, 8997-9004.	3.2	24

#	Article	IF	CITATIONS
55	Structural Characterization of Intramolecular Hg2+ Transfer between Flexibly Linked Domains of Mercuric Ion Reductase. Journal of Molecular Biology, 2011, 413, 639-656.	4.2	24
56	Displacement of OmpF loop 3 is not required for the membrane translocation of colicins N and A in vivo. FEBS Letters, 1998, 432, 117-122.	2.8	22
57	High coverage fluid-phase floating lipid bilayers supported by ï‰-thiolipid self-assembled monolayers. Journal of the Royal Society Interface, 2014, 11, 20140447.	3.4	22
58	Unexpected Effects of Gene Deletion on Interactions of Mercury with the Methylation-Deficient Mutant Δ <i>hgcAB</i> . Environmental Science and Technology Letters, 2014, 1, 271-276.	8.7	22
59	L-Arabinose Binding, Isomerization, and Epimerization by D-Xylose Isomerase: X-Ray/Neutron Crystallographic and Molecular Simulation Study. Structure, 2014, 22, 1287-1300.	3.3	22
60	Protein Kinase A Catalytic Subunit Primed for Action: Time-Lapse Crystallography of Michaelis Complex Formation. Structure, 2015, 23, 2331-2340.	3.3	22
61	Quantitative Proteomic Analysis of Biological Processes and Responses of the Bacterium <i>Desulfovibrio desulfuricans</i> ND132 upon Deletion of Its Mercury Methylation Genes. Proteomics, 2018, 18, e1700479.	2.2	22
62	Conformational Dynamics of AcrA Govern Multidrug Efflux Pump Assembly. ACS Infectious Diseases, 2019, 5, 1926-1935.	3.8	21
63	Development of CHARMM-Compatible Force-Field Parameters for Cobalamin and Related Cofactors from Quantum Mechanical Calculations. Journal of Chemical Theory and Computation, 2018, 14, 784-798.	5.3	20
64	Kinetics of Enzymatic Mercury Methylation at Nanomolar Concentrations Catalyzed by HgcAB. Applied and Environmental Microbiology, 2019, 85, .	3.1	20
65	Structure and Dynamics of a Compact State of a Multidomain Protein, the Mercuric Ion Reductase. Biophysical Journal, 2014, 107, 393-400.	0.5	19
66	The Two-State Prehensile Tail of the Antibacterial Toxin Colicin N. Biophysical Journal, 2017, 113, 1673-1684.	0.5	18
67	Co(salen)-Catalyzed Oxidation of Lignin Models to Form Benzoquinones and Benzaldehydes: A Computational and Experimental Study. ACS Sustainable Chemistry and Engineering, 2020, 8, 7225-7234.	6.7	18
68	Emerging investigator series: methylmercury speciation and dimethylmercury production in sulfidic solutions. Environmental Sciences: Processes and Impacts, 2018, 20, 584-594.	3.5	17
69	Hit Expansion of a Noncovalent SARS-CoV-2 Main Protease Inhibitor. ACS Pharmacology and Translational Science, 2022, 5, 255-265.	4.9	17
70	Mycolyltransferase from Mycobacterium tuberculosis in covalent complex with tetrahydrolipstatin provides insights into antigen 85 catalysis. Journal of Biological Chemistry, 2018, 293, 3651-3662.	3.4	16
71	Mechanistic Duality of Bacterial Efflux Substrates and Inhibitors: Example of Simple Substituted Cinnamoyl and Naphthyl Amides. ACS Infectious Diseases, 2021, 7, 2650-2665.	3.8	16
72	Modeling of the Passive Permeation of Mercury and Methylmercury Complexes Through a Bacterial Cytoplasmic Membrane. Environmental Science & Technology, 2017, 51, 10595-10604.	10.0	15

#	Article	IF	CITATIONS
73	Hyperconjugation Promotes Catalysis in a Pyridoxal 5′-Phosphate-Dependent Enzyme. ACS Catalysis, 2018, 8, 6733-6737.	11.2	15
74	Hepatitis C Virus NS5B Polymerase:  QM/MM Calculations Show the Important Role of the Internal Energy in Ligand Binding. Journal of Physical Chemistry B, 2008, 112, 3168-3176.	2.6	14
75	Antibacterial toxin colicin N and phage protein G3p compete with TolB for a binding site on TolA. Microbiology (United Kingdom), 2015, 161, 503-515.	1.8	14
76	Quantum Chemical Approach for Calculating Stability Constants of Mercury Complexes. ACS Earth and Space Chemistry, 2018, 2, 1168-1178.	2.7	14
77	Comparative Informatics Analysis to Evaluate Site-Specific Protein Oxidation in Multidimensional LC–MS/MS Data. Journal of Proteome Research, 2013, 12, 3307-3316.	3.7	13
78	Insight into the Catalytic Mechanism of GH11 Xylanase: Computational Analysis of Substrate Distortion Based on a Neutron Structure. Journal of the American Chemical Society, 2020, 142, 17966-17980.	13.7	13
79	Lpp positions peptidoglycan at the AcrA-TolC interface in the AcrAB-TolC multidrug efflux pump. Biophysical Journal, 2021, 120, 3973-3982.	0.5	13
80	Toward the rational design of macrolide antibiotics to combat resistance. Chemical Biology and Drug Design, 2017, 90, 641-652.	3.2	10
81	Modeling Mercury in Proteins. Methods in Enzymology, 2016, 578, 103-122.	1.0	9
82	Modular Protein Engineering Approach to the Functionalization of Gold Nanoparticles for Use in Clinical Diagnostics. ACS Applied Nano Materials, 2018, 1, 3590-3599.	5.0	9
83	Tuneable hydrogels of Caf1 protein fibers. Materials Science and Engineering C, 2018, 93, 88-95.	7.3	9
84	Antitumor T-cell Immunity Contributes to Pancreatic Cancer Immune Resistance. Cancer Immunology Research, 2021, 9, 386-400.	3.4	9
85	Property space mapping of Pseudomonas aeruginosa permeability to small molecules. Scientific Reports, 2022, 12, 8220.	3.3	9
86	Engineered mosaic protein polymers; a simple route to multifunctional biomaterials. Journal of Biological Engineering, 2019, 13, 54.	4.7	7
87	Induction of the immunoprotective coat of Yersinia pestis at body temperature is mediated by the Caf1R transcription factor. BMC Microbiology, 2019, 19, 68.	3.3	7
88	Combining Three-Dimensional Modeling with Artificial Intelligence to Increase Specificity and Precision in Peptide–MHC Binding Predictions. Journal of Immunology, 2020, 205, 1962-1977.	0.8	7
89	HackaMol: An Object-Oriented Modern Perl Library for Molecular Hacking on Multiple Scales. Journal of Chemical Information and Modeling, 2015, 55, 721-726.	5.4	6
90	Longâ€Range Electrostaticsâ€Induced Twoâ€Proton Transfer Captured by Neutron Crystallography in an Enzyme Catalytic Site. Angewandte Chemie, 2016, 128, 5008-5011.	2.0	6

#	Article	IF	CITATIONS
91	Pseudobond parameters for QM/MM studies involving nucleosides, nucleotides, and their analogs. Journal of Chemical Physics, 2013, 138, 045102.	3.0	5
92	Horizontal transfer of a pathway for coumarate catabolism unexpectedly inhibits purine nucleotide biosynthesis. Molecular Microbiology, 2019, 112, 1784-1797.	2.5	5
93	A Minimal Membrane Metal Transport System: Dynamics and Energetics of <i>mer</i> Proteins. Journal of Computational Chemistry, 2020, 41, 528-537.	3.3	5
94	Studying the surfaces of bacteria using neutron scattering: finding new openings for antibiotics. Biochemical Society Transactions, 2020, 48, 2139-2149.	3.4	5
95	Core cysteine residues in the Plasminogen-Apple-Nematode (PAN) domain are critical for HGF/c-MET signaling. Communications Biology, 2022, 5, .	4.4	5
96	Ligand-Dependent Sodium Ion Dynamics within the A _{2A} Adenosine Receptor: A Molecular Dynamics Study. Journal of Physical Chemistry B, 2019, 123, 7947-7954.	2.6	4
97	A probabilistic perspective on thermodynamic parameter uncertainties: Understanding aqueous speciation of mercury. Geochimica Et Cosmochimica Acta, 2019, 263, 108-121.	3.9	4
98	Toward Quantitatively Accurate Calculation of the Redox-Associated Acid–Base and Ligand Binding Equilibria of Aquacobalamin. Journal of Physical Chemistry B, 2016, 120, 7307-7318.	2.6	3
99	The AQUAâ€MER databases and aqueous speciation server: A web resource for multiscale modeling of mercury speciation. Journal of Computational Chemistry, 2020, 41, 147-155.	3.3	3
100	Probing the oligomeric re-assembling of bacterial fimbriae in vitro: a small-angle X-ray scattering and analytical ultracentrifugation study. European Biophysics Journal, 2021, 50, 597-611.	2.2	3
101	Mechanistic Investigation of Dimethylmercury Formation Mediated by a Sulfide Mineral Surface. Journal of Physical Chemistry A, 2021, 125, 5397-5405.	2.5	3
102	Pretreatment with Sodium Methyl Mercaptide Increases Carbohydrate Yield during Kraft Pulping. ACS Sustainable Chemistry and Engineering, 2021, 9, 11571-11580.	6.7	3
103	Helix N-Cap Residues Drive the Acid Unfolding That Is Essential in the Action of the Toxin Colicin A. Biochemistry, 2019, 58, 4882-4892.	2.5	1
104	Hotspot Coevolution Is a Key Identifier of Near-Native Protein Complexes. Journal of Physical Chemistry B, 2021, 125, 6058-6067.	2.6	1
105	Macromolecular organisation of recombinant Yersinia pestis F1 antigen and the effect of structure on immunogenicity. FEMS Immunology and Medical Microbiology, 1998, 21, 213-221.	2.7	1
106	Mercury Detoxification by Bacteria: Simulations of Transcription Activation and MercuryCarbon Bond Cleavage. , 2011, , 311-324.		0
107	Molecular Simulation in the Energy Biosciences. RSC Biomolecular Sciences, 2012, , 87-114.	0.4	0
108	Editorial: Advances in computational molecular biophysics. Biochimica Et Biophysica Acta - General Subjects, 2021, 1865, 129888.	2.4	0

#	Article	IF	CITATIONS
109	OpenMDIr: parallel, open-source tools for general protein structure modeling and refinement from pairwise distances. Bioinformatics, 2022, 38, 3297-3298.	4.1	0